

# Optimal Control for Generating Quantum Gates in Open Dissipative Systems

T. Schulte-Herbrüggen,<sup>1,\*</sup> A. Spörl,<sup>1</sup> N. Khaneja,<sup>2</sup> and S.J. Glaser<sup>1</sup>

<sup>1</sup>*Department of Chemistry, Technical University Munich,  
Lichtenbergstrasse 4, D-85747 Garching, Germany*

<sup>2</sup>*Division of Applied Sciences, Harvard University, Cambridge MA02138, USA*

(Dated: 24th November 2018)

Optimal control methods for implementing quantum modules with least amount of dissipation are devised to give best approximations to unitary gates under explicit relaxation. They are the methods of choice to govern quantum systems within decoherence-poor subspaces whenever the drift Hamiltonian would otherwise sweep the system through decoherence-rich states of the embedding larger Liouville space. Superoperator GRAPE derived controls outperform Trotter-type approaches significantly: in a standard model system encoding two logical qubits by four physical ones, one obtains a CNOT with fidelities beyond 95% instead of at most 15 % in the Trotter limit with the additional benefit of the former requiring control fields orders of magnitude lower than the latter.

PACS numbers: 03.67.-a, 03.67.Lx, 03.65.Yz, 03.67.Pp; 82.56.Jn

## I. INTRODUCTION

Using experimentally controllable quantum systems to perform computational tasks or to simulate the behaviour of other quantum systems [1, 2] is promising: by exploiting quantum coherences, one may reduce the complexity of the problem when going from a classical setting to a quantum setting. Protecting quantum systems against relaxation (“decoherence”) is therefore tantamount to using coherent quantum superpositions as a key resource. To this end, decoherence-free subspaces have been applied [3], bang-bang controls [4, 5, 6] have been used for decoupling the system from dissipative interaction with the environment, while a quantum Zeno approach [7] may be taken to projectively keep the system within the desired subspace [8]. Controlling decoherence is thus an important yet demanding task, for an overview see e.g. Ref. [9, 10]. The problem of implementing quantum gates or quantum modules experimentally is even more challenging: one has to fight decoherence while simultaneously steering the quantum system with all its basis states into a linear image of maximal overlap with the desired target gate.

Recently, we have shown how near time-optimal control by GRAPE [11] take pioneering realisations from their fidelity-limit to the decoherence-limit [12].

In spectroscopy, optimal control helps to keep state transfer along slowly relaxing directions of the Liouville space [13]. However, in quantum computing, the entire basis has to be transformed. This precludes naive adaptation to the entire Liouville space, since the gain of going along protected dimensions is outweighed by losses in the orthocomplement. Yet embedding the logical qubit system as a decoherence-protected system into a larger Liouville space of the encoding physical system raises the question to which extent the target module is controllable

within the protected subspace by admissible controls.

In this category of setting, the new superoperator gradient algorithm will turn out to be particularly powerful to give best approximations to unitary target gates in dissipative quantum systems thus extending the toolbox of quantum control, see e.g. [11, 14, 15, 16, 17, 18, 19, 20].

## II. CONTROLLABILITY OF OPEN QUANTUM SYSTEMS

In the model systems studied below, we will use systems that are *fully controllable* [21, 22, 23, 24, 25, 26], i.e. those in which—neglecting decoherence—for any initial density operator  $\rho$ , the entire unitary orbit  $U(\rho) := \{U\rho U^{-1} \mid U \text{ unitary}\}$  can be reached [27] by evolutions under the system Hamiltonian (drift) and the experimentally admissible controls. However, we will see that certain tasks can be performed within a subspace, e.g. a subspace protected totally or partially against dissipation explicitly given in the equation of motion.

### A. Equations of Motion

Generating unitary modules for quantum computation requires synthesising a simultaneous linear image of all the basis states spanning the Hilbert space or subspace on which the gates shall act. It thus generalises the spectroscopic task to transfer the state of a system from a given initial one into maximal overlap with a desired target state. The control problem of maximising this overlap subject to the dynamics being governed by Schrödinger’s equation (for states of closed systems represented in Hilbert space) or by Liouville’s equation (for density operators of potentially open systems represented in the so-called Liouville space)

$$|\dot{\psi}\rangle = -iH|\psi\rangle \quad (1)$$

$$\dot{\rho} = -i[H, \rho] \equiv -i\text{ad}_H(\rho) \quad (2)$$

\*Electronic address: tosh@ch.tum.de

may be addressed by our algorithm GRAPE [11]. Using the notation  $\text{Ad}_U(\cdot) := U(\cdot)U^\dagger$ , the corresponding operator equations

$$\dot{U} = -iH U \quad (3)$$

$$\dot{\text{Ad}}_U = -i \text{ad}_H \circ \text{Ad}_U \quad (4)$$

can be used in quantum control in order to realise quantum gates  $U(T)$  with maximum trace fidelities  $\text{Retr}\{U_{\text{target}}^\dagger U(T)\}$  in case overall global phases shall be respected, or  $\text{Retr}\{\text{Ad}_{U_{\text{target}}}^\dagger \text{Ad}_{U(T)}\}$  if the global phase is immaterial [19].

Likewise, the corresponding Master equations for state transfer or gate synthesis read

$$\dot{\rho} = -(i \text{ad}_H + \Gamma) \rho \quad (5)$$

$$\dot{F}_{\text{Ad}_U} = -(i \text{ad}_H + \Gamma) \circ F_{\text{Ad}_U} \quad , \quad (6)$$

respectively, where  $\Gamma$  may take the usual Lindblad form

$$\Gamma(\rho) = \frac{1}{2} \sum_k \{2 V_k^\dagger \rho V_k - V_k^\dagger V_k \rho - \rho V_k^\dagger V_k\} \quad . \quad (7)$$

$F_{\text{Ad}_U}$  denotes the contractive linear image of all basis states of the Liouville space representing the open system. Its dynamics are governed by the superoperator Eqn. 6 to the Master Eqn. 5. With these stipulations, the GRAPE algorithm can be lifted to the superoperator level in order to cope with the dynamics of open systems.

## B. Controllability of the Model Systems

For comparing the power of optimal control for protection from decoherence, we build upon the usual encoding of one logical qubit in two physical ones  $|0\rangle_L = |\psi^+\rangle$  and  $|1\rangle_L = |\psi^-\rangle$ . Four Bell basis elements then span an operator subspace protected against  $T_2$ -type relaxation  $\mathcal{B} := \text{span}\{|\psi^\pm\rangle\langle\psi^\pm|, |\psi^\mp\rangle\langle\psi^\pm|\}$ , as for any  $\rho \in \mathcal{B}$ , in the slow-tumbling limit of the Bloch-Redfield relaxation [33]  $\Gamma(\rho) := [A_{00}^\dagger, [A_{00}, \rho]] = [zz, [zz, \rho]] = 0$ . If the two are coupled by a Heisenberg-XX interaction and the controls take the form of local  $z$ -pulses acting on the two qubits simultaneously with opposite sign, one obtains the usual fully controllable logical single qubit over  $\mathcal{B}$ , since

$$\langle\{(xx + yy), (z\mathbb{1} - \mathbb{1}z), (yx - xy)\}\rangle \stackrel{\text{iso}}{=} \mathfrak{su}(2) \quad , \quad (8)$$

where  $\langle \cdot \rangle$  denotes the generating set obtained by commutation.

As in Refs. [28, 29, 30], one gets a fully controllable logical two-spin system by coupling two of the above qubit pairs with an Ising-ZZ interaction, thus forming our reference *System-I* defined by the drift Hamiltonian  $D_1$  and the controls  $C_{1,2}$  (with non-zero  $J_{xx}$  and  $J_{zz}$ )

$$D_1 := J_{xx} (xx\mathbb{1}\mathbb{1} + \mathbb{1}\mathbb{1}xx + yy\mathbb{1}\mathbb{1} + \mathbb{1}\mathbb{1}yy) + J_{zz} \mathbb{1}zz\mathbb{1} \quad (9)$$

$$C_1 := z\mathbb{1}\mathbb{1}\mathbb{1} - \mathbb{1}z\mathbb{1}\mathbb{1} \quad (10)$$

$$C_2 := \mathbb{1}\mathbb{1}z\mathbb{1} - \mathbb{1}\mathbb{1}1z \quad . \quad (11)$$

$$\text{Hence, } \langle\{D_1, C_1, C_2\}\rangle \stackrel{\text{iso}}{=} \mathfrak{su}(4) \quad (12)$$

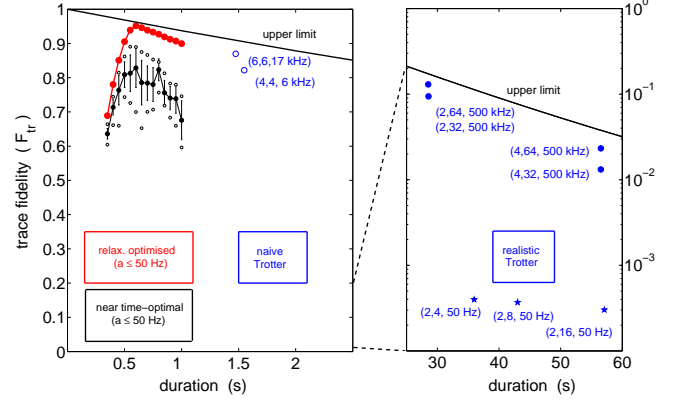


Figure 1: (Colour online) Fidelity of a CNOT gate realized by four physical qubits in different approaches: (●) by numerical optimal control under explicit relaxation; (●) by tracking near time-optimal controls showing widely scattered quality factors with the intervals giving mean  $\pm$  standard deviation for all the 15 control sequences tested (○ for best and worst values); (○) by naive Trotter calculations assuming to every interaction the inverse is directly obtainable; (●) by a realistic Trotter approach, where the inverse has to be explicitly generated. The numbers in brackets give the expansion coefficients  $n_{1,2}$  of Fig. 3 and the max. control amplitudes. The upper limit is imposed by slow  $T_1$ -type relaxation (see text). Without relaxation, all the Trotter sequences would achieve fidelities between 93 and 99 %, except (\*) the ones limited to control fields of amplitudes  $a \leq 50$  Hz: they fall below 5%.

in the following sense: at the cost of being reducible, this four-qubit encoding is a representation of  $\mathfrak{su}(4)$  restricted to the Liouville subspace  $\mathcal{B} \otimes \mathcal{B}$  spanning the states that are protected against  $T_2$ -type relaxation.

By extending the Ising-ZZ coupling between the two qubit pairs to an isotropic Heisenberg-XXX interaction, one gets what we define as *System-II*. Its drift term

$$D_1 + D_2 := J_{xx} (xx\mathbb{1}\mathbb{1} + \mathbb{1}\mathbb{1}xx + yy\mathbb{1}\mathbb{1} + \mathbb{1}\mathbb{1}yy) + J_{xyz} (\mathbb{1}xx\mathbb{1} + \mathbb{1}yy\mathbb{1} + \mathbb{1}zz\mathbb{1}) \quad (13)$$

takes the system out of the decoherence protected subspace, since the dynamics finds its Lie-algebraic closure in a 66-dimensional Lie algebra

$$\dim\langle\{(D_1 + D_2), C_1, C_2\}\rangle = 66 \quad , \quad (14)$$

to which  $\mathfrak{su}(4)$  is but a subalgebra.

Moreover, note that  $e^{-i\pi C_1}(D_1 + D_2)e^{i\pi C_1} = D_1 - D_2$ . So invoking Trotter's formula

$$\lim_{n \rightarrow \infty} (e^{-i(D_1 + D_2)/(2n)} e^{-i(D_1 - D_2)/(2n)})^n = e^{-iD_1} \quad (15)$$

it is easy to see that the dynamics of System-II may reduce to the subspace of System-I in the limit of infinitely many switchings between controls  $C_{1,2}$  and free evolution under  $(D_1 + D_2)$ . It is in this “decoupling limit” that System-II can also encode a fully controllable logical two-qubit system over the protected basis  $\mathcal{B} \otimes \mathcal{B}$ .

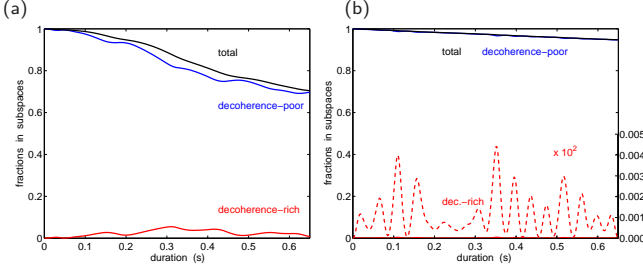


Figure 2: (Colour online) (a) Time evolution of all the protected basis states under a typical time-optimised control of Fig.1. Projections into the decoherence-poor and decoherence-rich parts of the Liouville space are shown. (b) Same for the new decoherence-protected controls. The system then stays almost entirely within the decoherence-poor subspace.

In the following paragraph we may thus compare the numerical results of decoherence-protection by optimal control with alternative pulse sequences derived by paper and pen exploiting the Trotter limit. As an example we choose the CNOT gate in a logical two-qubit system encoded in the protected four-qubit Bell basis  $\mathcal{B} \otimes \mathcal{B}$ .

### III. EXEMPLIFICATION BY MODEL SYSTEMS

For the sake of being more realistic, the model relaxation superoperator mimicking dipole-dipole relaxation within the two spin pairs in the sense of Bloch-Redfield theory is extended from covering solely  $T_2$ -type dissipation to mildly including  $T_1$  processes by taking (for each basis state  $\rho$ ) the sum [31]

$$\Gamma(\rho) := \sum_{m_1, m_2=-1}^1 [A_{2, (m_1, m_2)}^\dagger, [A_{2, (m_1, m_2)}, \rho]], \quad (16)$$

in which the contribution by the 0-order tensor  $A_{2, (0,0)} \sim zz$  is then scaled 100 times stronger than the new terms. So the resulting model relaxation rate constants finally become  $T_2^{-1} : T_1^{-1} = 4.027 \text{ s}^{-1} : 0.024 \text{ s}^{-1} \simeq 170 : 1$ , while the coupling constants are set to  $J_{xx} = 2 \text{ Hz}$  and  $J_{xyz} = J_{zz} = 1 \text{ Hz}$ .

Thus knowing the Master equation explicitly, four scenarios of approximating the CNOT gate as target are compared in Fig. 1. With decoherence-protected numerically optimised controls one obtains a fidelity beyond 95 %, while near time-optimal controls show a broad scattering: among the family of 15 sequences generated, serendipity may help some of them to reach a quality near 90 %, while others perform as bad as giving 65 %. Fig. 2 then elucidates how the new decoherence avoiding controls keep the system almost perfectly within the decoherence-poor subspace, whereas conventional near time-optimal controls partly sweep through the rich subspace thus suffering from relaxation.

Algebraic alternatives to numerical methods of optimal control exploit Trotter's formula for remaining within

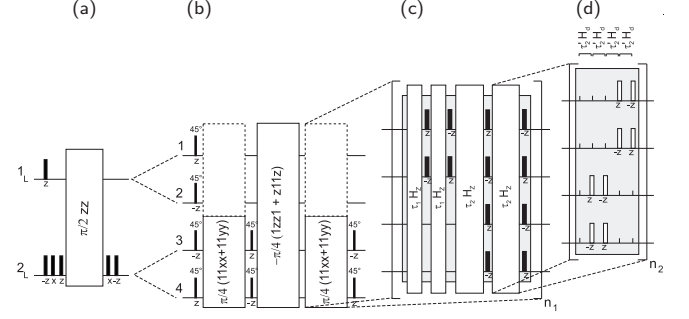


Figure 3: Alternative to numerical control: tedious algebraic derivation of controls for a CNOT in the decoherence-poor subspace taken from (a) the logical two-qubit system via (b) the encoded schematic physical four-qubit system to the physical realisations in the settings of (c) System-I and (d) System-II. Black bars are local  $\pi/2$ -pulses with phases given as subscript (other rotation angles given above); empty bars denote local  $z$ -rotations by flip angle  $\pi$ . Effective Hamiltonians  $\tau H$  are represented by large frames;  $n_1, n_2$  indicate repetitions for the respective Trotter expansions. The interior effective Hamiltonian in (b) requires even more complicated expansions.

the decoherence-poor subspace when realising the target CNOT. Though straightforward, they soon become unhandy as shown in Fig. 3. Assuming for the moment that to any evolution under a drift  $H_d$  the inverse evolution under  $-H_d$  is directly available, the corresponding “naive” expansions are of less than 3 times the length of the numerical results, yet requiring much stronger control fields (1 – 17 KHz instead of 50 Hz) as shown in Fig. 1. In practice, however, the inverse is often not immediately reachable, but will require waiting for periodicity. E.g. in System-II, the drift Hamiltonian shows eigenvalues that are relatively prime thus lacking periodicity altogether. When shifting the coupling to  $J_{xx} = 2.23 \text{ Hz}$  to introduce a favourable quasi-periodicity, one obtains almost perfect projection ( $F_{\text{tr}} \geq 1 - 10^{-10}$ ) onto the inverse drift evolution of System-II  $U^{-1} := e^{+i\frac{\pi}{4}H(D_1+D_2)}$  after 3.98 sec and onto  $-U^{-1}$  after 1.99 sec. Due to the latter, the identity  $\text{Ad}_{(-U^{-1})} = \text{Ad}_{(U^{-1})}$  [34] may be exploited to cut the duration for evolution under  $U^{-1}$  to 1.99 sec. Yet, even with these facilitations, the total length required for a realistic Trotter decomposition (with an overall trace fidelity of  $F_{\text{tr}} \geq 94.1 \%$  in the absence of decoherence) amounts to some 28.5 sec as shown in Fig. 1. Moreover, as soon as one includes very mild  $T_1$ -type processes, the relaxation rate constants in the decoherence-protected subspace are no longer strictly zero (as for pure  $T_2$ -type relaxation), but cover the interval  $[0.019 \text{ s}^{-1}, 0.060 \text{ s}^{-1}]$ . Consequently, a Trotter expansion lasting some 28.5 sec finally gives, under these realistic conditions, no more than 15% fidelity, while the new numerical methods allow for realisations beyond 95% fidelity in the same setting (even with the original parameter  $J_{xx} = 2.0 \text{ Hz}$ ).

#### IV. CONCLUSION

We have provided optimal-control tools to systematically find near optimal approximations to (projective) unitary target gates by superoperators that are the contractive linear image of an entire basis set for the respective open quantum system encoding logical qubits. This goes beyond the unitary superoperators [31, 32] used recently in quantum control [19, 20]. The progress is quantified in a typical model system of four physical qubits encoding two logical ones: when the Master equation is known, the new method is systematic and significantly superior to near time-optimal realisations, which in turn are but a guess when the dissipation process cannot be quantitatively characterised. In this case, generating a set of  $10 - 20$  such near time-optimal control sequences and testing them empirically is required for getting acceptable results with more confidence, yet on the basis of trial and error. As follows by controllability analysis, Trotter-type expansions allow for realisations within decoherence-poor subspaces in the limit of infinitely many switchings. However, in realistic set-

tings for obtaining inverse interactions, they become so lengthy that they only work in the idealised limit of both  $T_2$  and  $T_1$ -decoherence-free subspaces, but fail as soon as very mild  $T_1$ -relaxation processes are taken into account.

The new optimal control tools are therefore the method of choice in systems with explicitly known relaxation superoperators. Being applicable to spin and pseudo-spin systems, they are anticipated to find broad use for fighting decoherence in practical quantum control. In order to fully exploit the power of optimal control of open systems the challenge is shifted to (i) thoroughly understanding the relaxation mechanisms pertinent to the concrete quantum hardware architecture and (ii) being able to determine the relaxation parameters to sufficient accuracy.

#### Acknowledgments

This work was supported in part by the integrated EU project QAP as well as by *Deutsche Forschungsgemeinschaft*, DFG, in the incentive QIV.

---

[1] R. P. Feynman, *Int. J. Theo. Phys.* **21**, 467 (1982).  
[2] R. P. Feynman, *Feynman Lectures on Computation* (Perseus Books, Reading, MA., 1996).  
[3] P. Zanardi and M. Rasetti, *Phys. Rev. Lett.* **79**, 3306 (1997).  
[4] L. Viola, E. Knill, and S. Lloyd, *Phys. Rev. Lett.* **82**, 2417 (1999).  
[5] L. Viola, E. Knill, and S. Lloyd, *Phys. Rev. Lett.* **83**, 4888 (1999).  
[6] L. Viola, E. Knill, and S. Lloyd, *Phys. Rev. Lett.* **85**, 3520 (2000).  
[7] B. Misra and E. Sudarshan, *J. Math. Phys.* **18**, 756 (1977).  
[8] P. Facchi and S. Pascazio, *Phys. Rev. Lett.* **89**, 080401 (2001).  
[9] D. Lidar and B. Whaley, *Irreversible Quantum Dynamics, Lect. Notes Phys.* (Springer, Berlin, 2003), vol. 622, chap. Decoherence-Free Subspaces and Subsystems, pp. 83–120.  
[10] P. Facchi, S. Tasaki, S. Pascazio, H. Nakazato, A. Tokuse, and D. Lidar, *Phys. Rev. A* **71**, 022302 (2005).  
[11] N. Khaneja, T. Reiss, C. Kehlet, T. Schulte-Herbrüggen, and S. J. Glaser, *J. Magn. Reson.* **172**, 296 (2005).  
[12] A. K. Spörl, T. Schulte-Herbrüggen, S. J. Glaser, V. Bergholm, M. J. Storcz, J. Ferber, and F. K. Wilhelm (2005), quant-ph/0504202.  
[13] N. Khaneja, B. Luy, and S. J. Glaser, *Proc. Natl. Acad. Sci. USA* **100**, 13162 (2003).  
[14] S. Lloyd, *Phys. Rev. A* **62**, 022108 (2000).  
[15] J. P. Palao and R. Kosloff, *Phys. Rev. Lett.* **89**, 188301 (2002).  
[16] J. J. García-Ripoll, P. Zoller, and J. I. Cirac, *Phys. Rev. Lett.* **91**, 157901 (2003).  
[17] Y. Ohtsuki, G. Turinici, and H. Rabitz, *J. Chem. Phys.* **120**, 5509 (2004).  
[18] S. E. Sklarz and D. J. Tannor (2004), quant-ph/0404081.  
[19] T. Schulte-Herbrüggen, A. K. Spörl, N. Khaneja, and S. J. Glaser, *Phys. Rev. A* **72**, 042331 (2005).  
[20] S. E. Sklarz and D. J. Tannor, *Chem. Phys.* **322**, 87 (2006).  
[21] V. Jurdjevic and H. Sussmann, *J. Diff. Equat.* **12**, 313 (1972).  
[22] H. Sussmann and V. Jurdjevic, *J. Diff. Equat.* **12**, 95 (1972).  
[23] R. W. Brockett, *SIAM J. Control* **10**, 265 (1972).  
[24] R. W. Brockett, *SIAM J. Appl. Math.* **25**, 213 (1973).  
[25] W. M. Boothby and E. N. Wilson, *SIAM J. Control Optim.* **17**, 212 (1979).  
[26] T. Schulte-Herbrüggen, *Aspects and Prospects of High-Resolution NMR* (PhD Thesis, Diss-ETH 12752, Zürich, 1998).  
[27] F. Albertini and D. D'Alessandro, *IEEE Trans. Automat. Control* **48**, 1399 (2003).  
[28] D. Lidar and L. Wu, *Phys. Rev. Lett.* **88**, 017905 (2002).  
[29] L. Wu and D. Lidar, *Phys. Rev. Lett.* **88**, 207902 (2002).  
[30] P. Zanardi and S. Lloyd, *Phys. Rev. A* **69**, 022313 (2004).  
[31] R. R. Ernst, G. Bodenhausen, and A. Wokaun, *Principles of Nuclear Magnetic Resonance in One and Two Dimensions* (Clarendon Press, Oxford, 1987).  
[32] C. N. Banwell and H. Primas, *Molec. Phys.* **6**, 225 (1963).  
[33] with the spin tensor  $A_{2,0} := \frac{1}{\sqrt{6}}(\frac{3}{2}zz - \mathbf{I}_1\mathbf{I}_2)$  [31], using the short-hand notation  $zz := \sigma_z \otimes \sigma_z/2$  and likewise henceforth  $\mathbf{1}_{\mu\nu}\mathbf{1} := \frac{1}{2}\mathbf{1}_2 \otimes \sigma_\mu \otimes \sigma_\nu \otimes \mathbf{1}_2$  for  $\mu, \nu \in \{x, y, z\}$ ;  
[34] Since  $\text{Ad}_U$  is a representation of the projective group  $PSU(N) := SU(N)/\mathbb{Z}_N$ , where  $\mathbb{Z}_N$  is the centre of  $SU(N)$ , one finds  $\text{Ad}_{(-U)} = \text{Ad}_U$  for all qubit dynamics by  $U \in SU(2^n)$  with  $n = 1, 2, \dots$ .